

Supporting Information

Restriction of telomerase capping by short non-toxic peptides via arresting telomeric G-quadruplex

Jagannath Jana, Pallabi Sengupta[€], Soma Mondal[€] and Subhrangsu Chatterjee*

P-1/12 CIT Scheme, Bose Institute, Department of Biophysics, Kolkata,-700054, India

€ -contributed equally

Figure Legends:

Figure S1: A plot of fluorescence intensity versus wavelength for FK13 binding to GQ23 shows a blue shift of 10 nm. 10 μ M of GQ23 was titrated with increasing concentration (0-40 μ M) of FK13.

Figure S2: A plot of $\Delta\lambda$ vs. concentration of FK13 showed binding of FK13 to GQ23 (A). An increase in Fluorescence Anisotropy with increasing concentration of GQ23 showed binding of KR12A (B), KR12B (C) and KR12C (D) to GQ23. 5 μ M of peptides were titrated with increasing concentration (0-20 μ M) of GQ23.

Figure S3: CD spectra of GQ23 in presence of increasing concentration of FK13 (A), KR12A (B), KR12B (C) and KR12C (D). 20 μ M of GQ23 was titrated with increasing concentration of peptides ranging from (0-60 μ M).

Figure S4: CD melting profile of free GQ23 (20 μ M).

Figure S5: CD melting temperature of free duplex (20 μ M) (A), duplex-FK13 (1:3) complex (B) and duplex DNA-(KR12A, KR12B and KR12C) (1:3) complex.

Figure S6: Isothermal Titration Calorimetry (ITC) profile of peptides binding to duplex DNA. FK13-duplex DNA binding (A), KR12A-duplex DNA binding (B), KR12B-duplex DNA binding (C) and KR12C-duplex DNA binding (D). The solid line represents the best fit data using 'three site binding model'

Figure S7: One dimensional imino proton resonance spectra of GQ23 (300 μ M) with increasing concentration of FK13 (0-900 μ M).

Figure S8: One-dimensional ³¹P-NMR spectrum of GQ23 (300 μ M) without FK13 and in the presence of increasing concentration of FK13 (0-900 μ M).

Figure S9: Secondary structures of peptides (20 μ M) in absence and presence of LPS (0-60 μ M) by Circular Dichromism. Far-UV CD spectra of peptides, FK13 (A), KR12A (B), KR12B (C) and KR12C (D) in the absence (red line) and the presence LPS (blue and violet line).

Figure S10: Fingerprint region of two-dimensional ^1H - ^1H NOESY spectra of peptides (1mM), FK13 (A), KR12A (B), KR12B (C) and KR12C (D) in LPS (5-25 μM).

Figure S11: Molecular dynamics simulation of GQ23 bound to FK13 at different time scales. 0 ns (A) and 40 ns (B).

Figure S12: A plot of RMSD of all atom vs time for GQ23 free (black line) and GQ23 bound to FK13 (red line).

Figure S13: Analysis of DNA content and cell cycle distribution in MCF-7 cells treated with FK13, KR12A, KR12B, and KR12C at 20 and 40 μM for 24 hours. Elevation in Sub G0 population is pronounced with increasing peptide concentration which corresponds to the apoptosis induction upon treatment. At 20 μM concentration of KR12A, KR12C and FK13, accumulation of G2/M phase is evident than the untreated cells with concomitant decline in G0/G1 and S phase. But an increase up to 40 μM , decreases G2/M phase population which is supported by concurrent hike in Sub G0 phase.

Figure S14: Confocal Microscopy images of MCF7 cell nucleus after 5 minutes incubation. DAPI (blue) stain nucleus (left panel). FITC (green) labelled FK13 showed no localization at nucleus of MCF7 cell (middle panel). No colocalization of DAPI and FITC-FK13 was observed (right panel).

Figure S15: Confocal Microscopy images of MCF7 cell nucleus after 24 hours incubation. DAPI stain nucleus (A). FITC labeled FK13 localised at nucleus of MCF7 cell (B). Colocalization of DAPI and FITC-FK13 (C).

Figure S1:

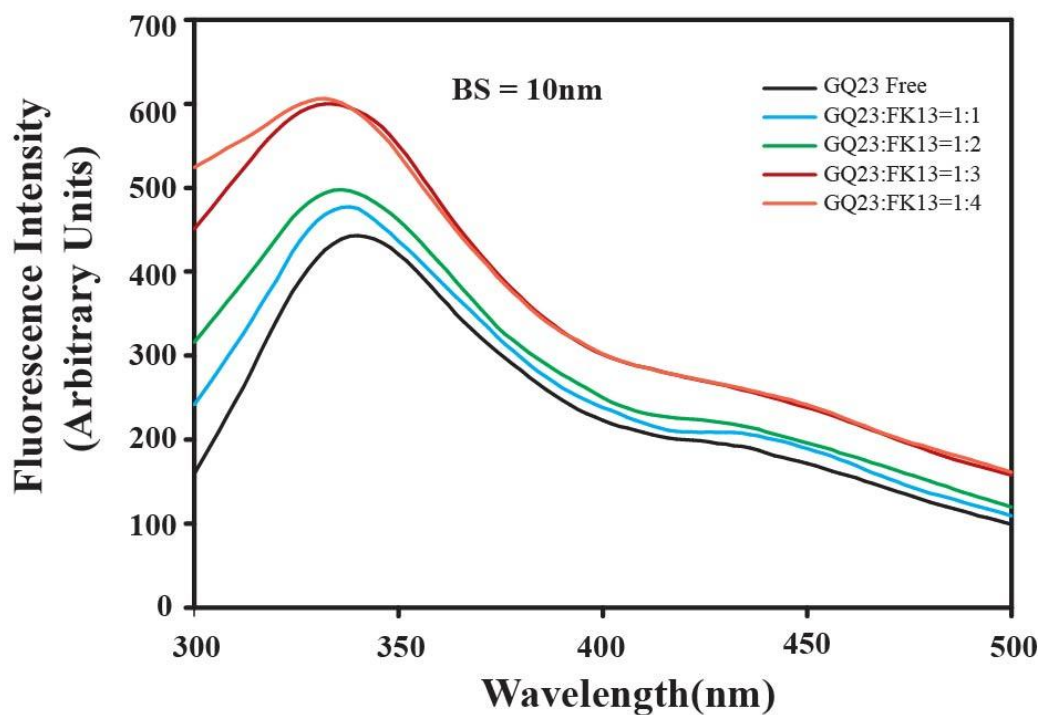


Figure S2:

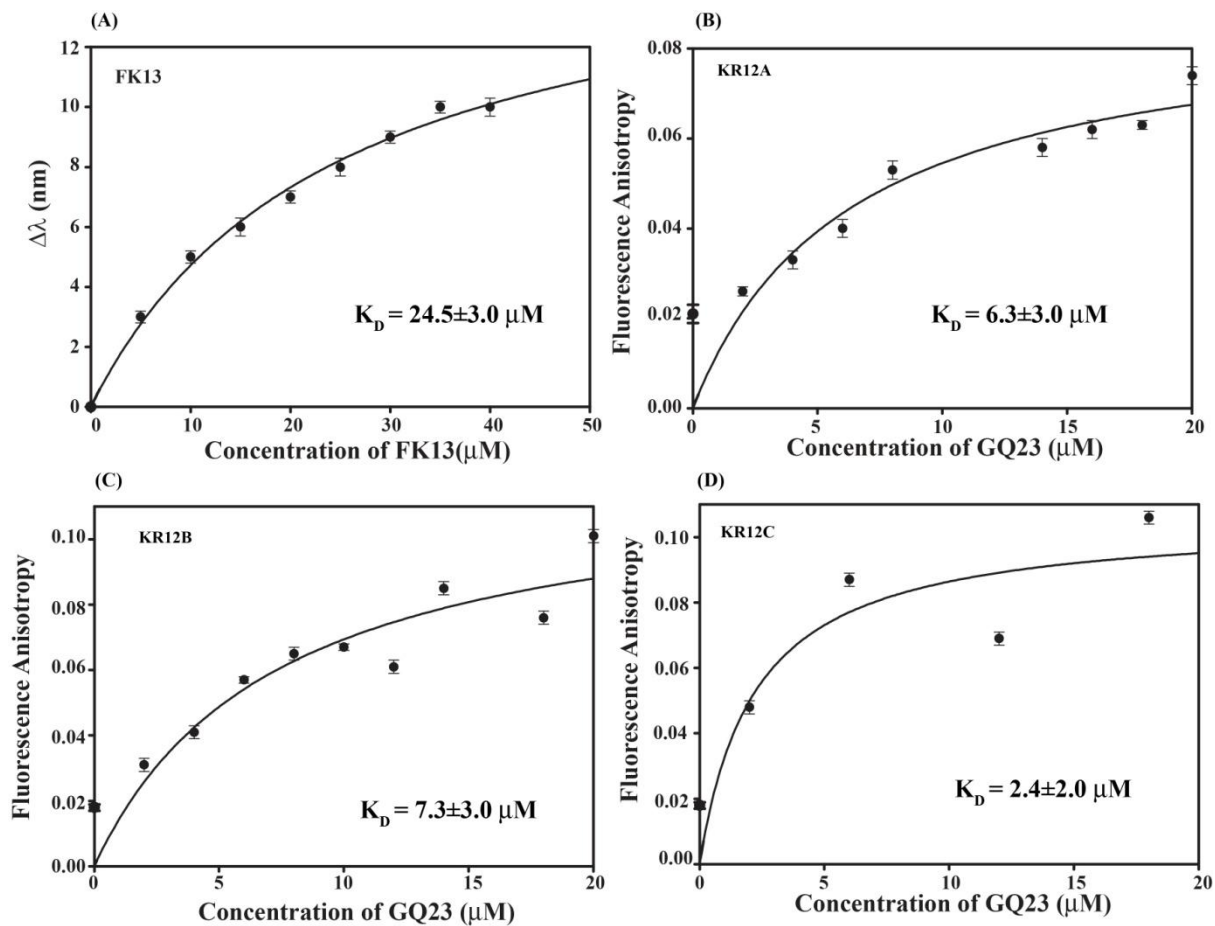


Figure S3:

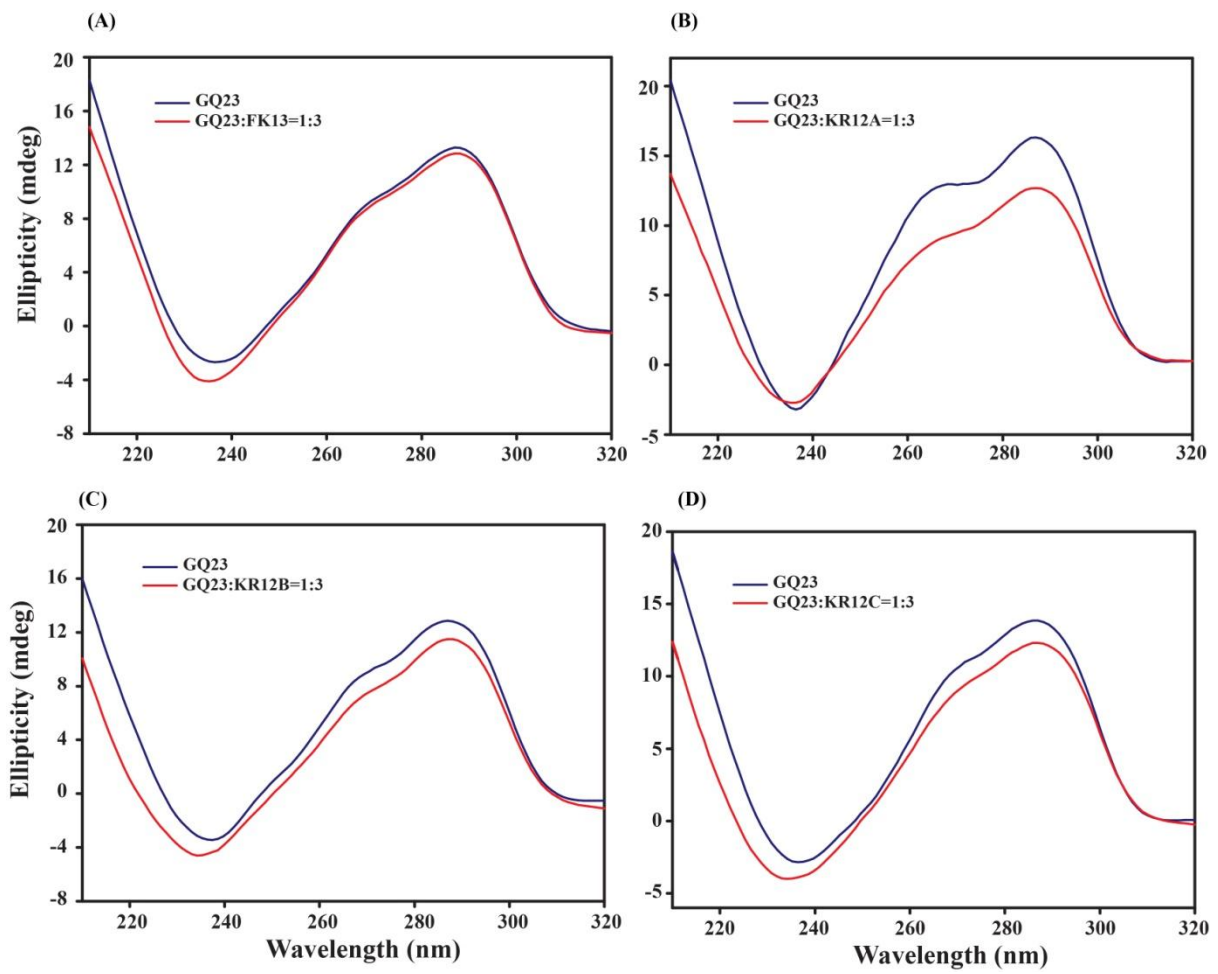


Figure S4:

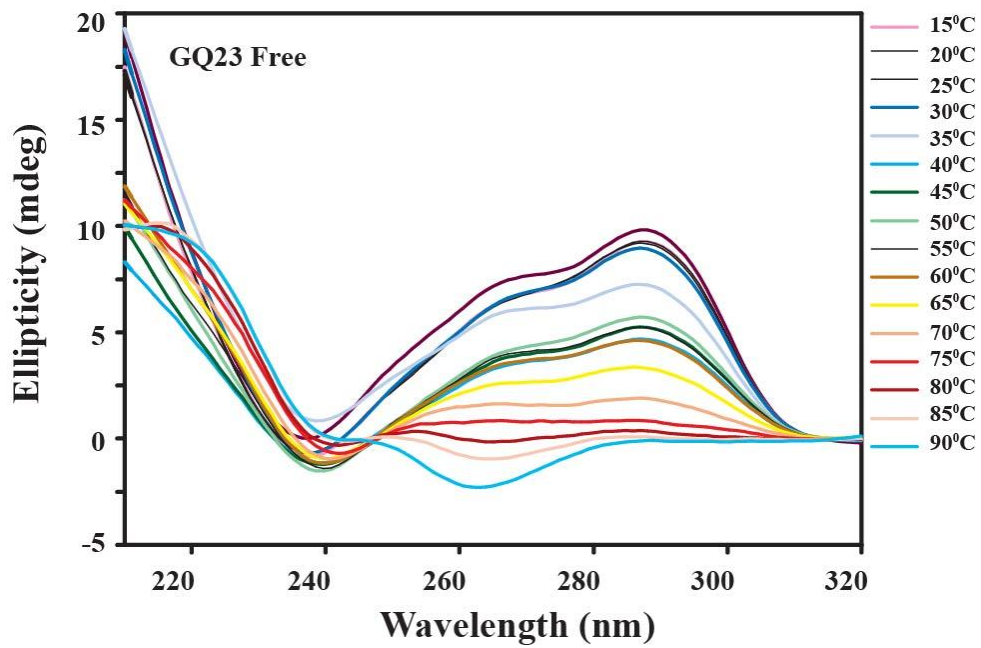


Figure S5:

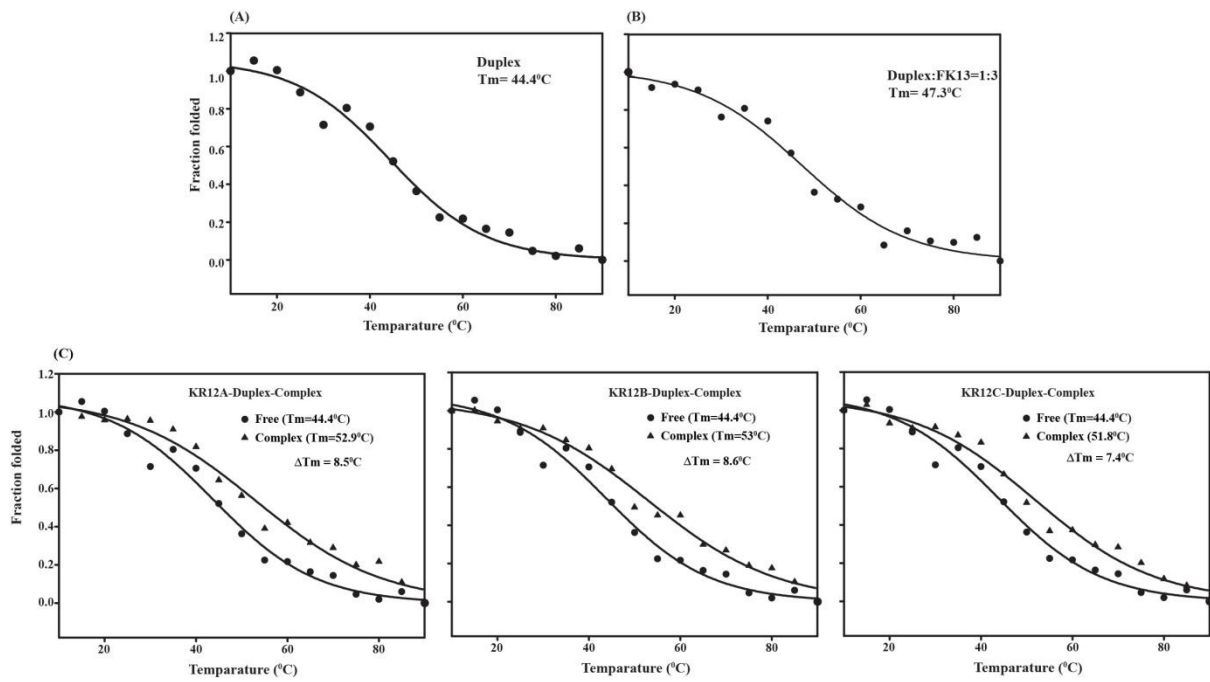


Figure S6:

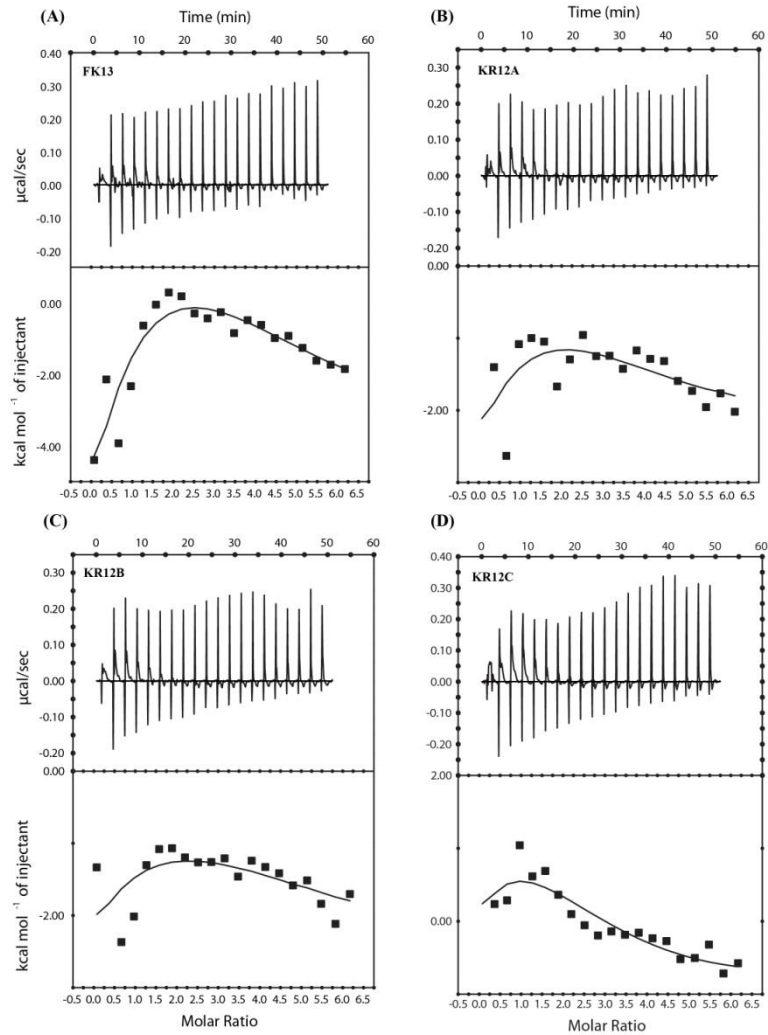


Figure S7:

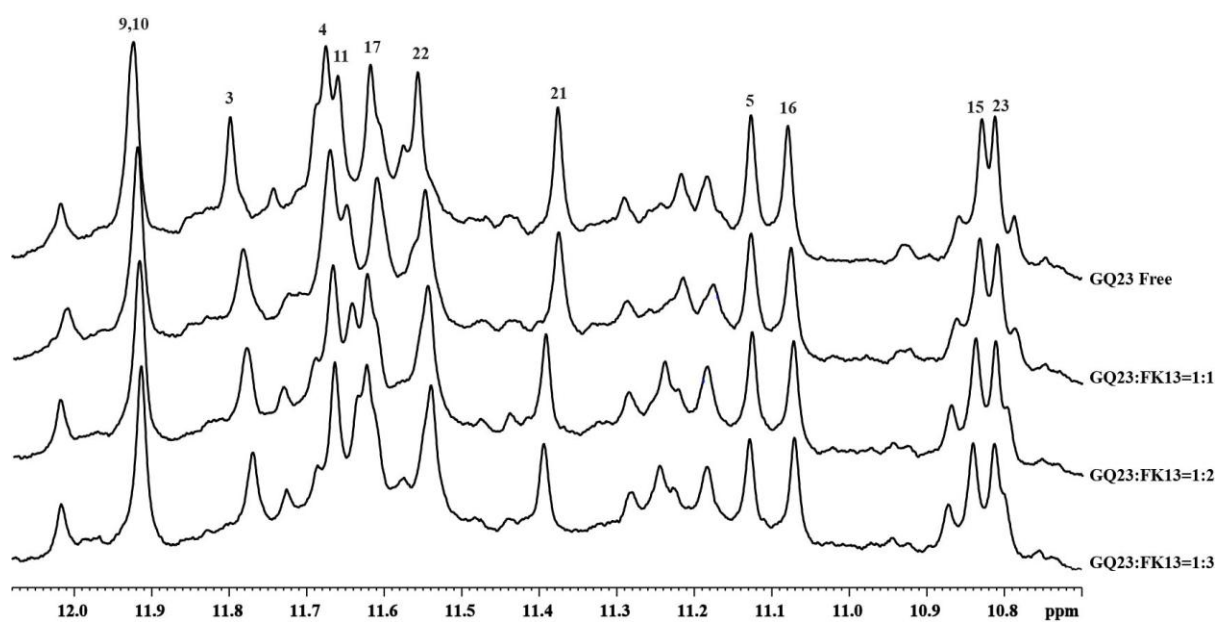


Figure S8:

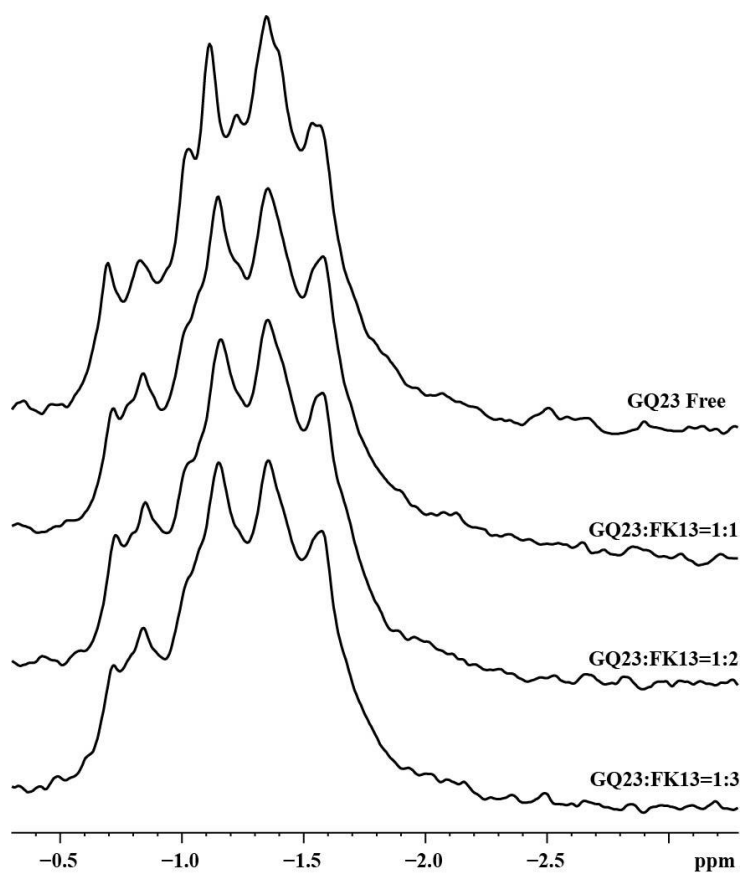


Figure S9:

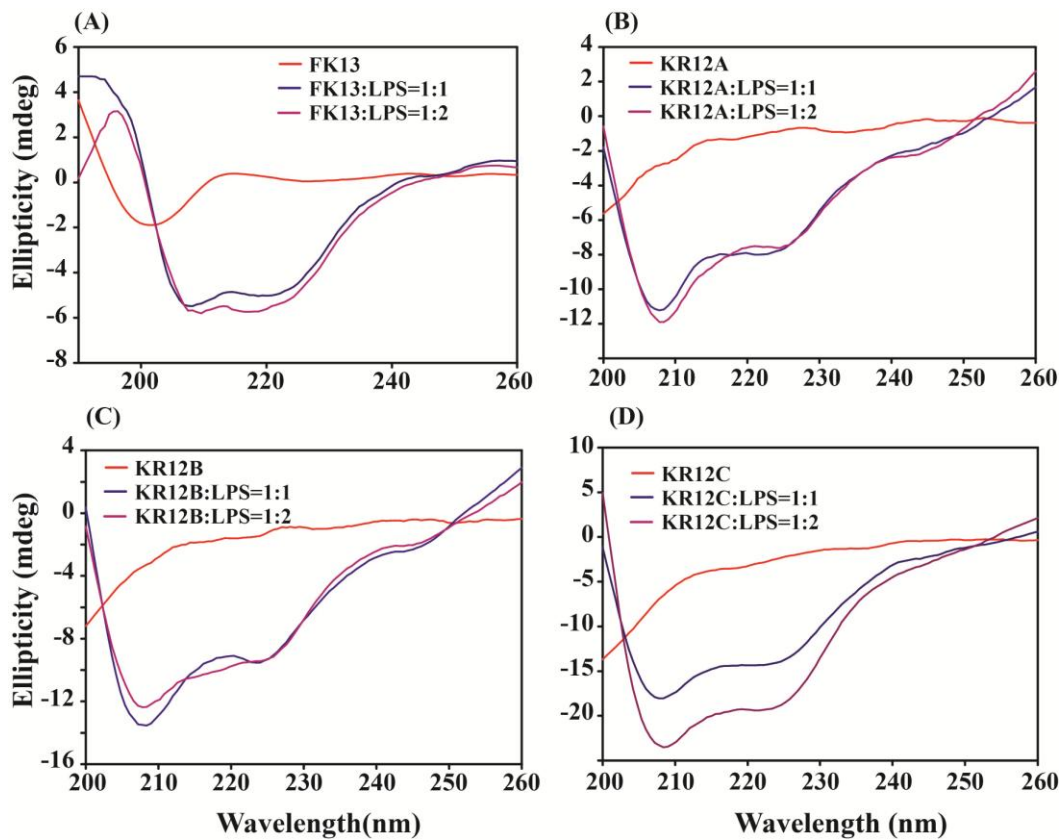


Figure S10:

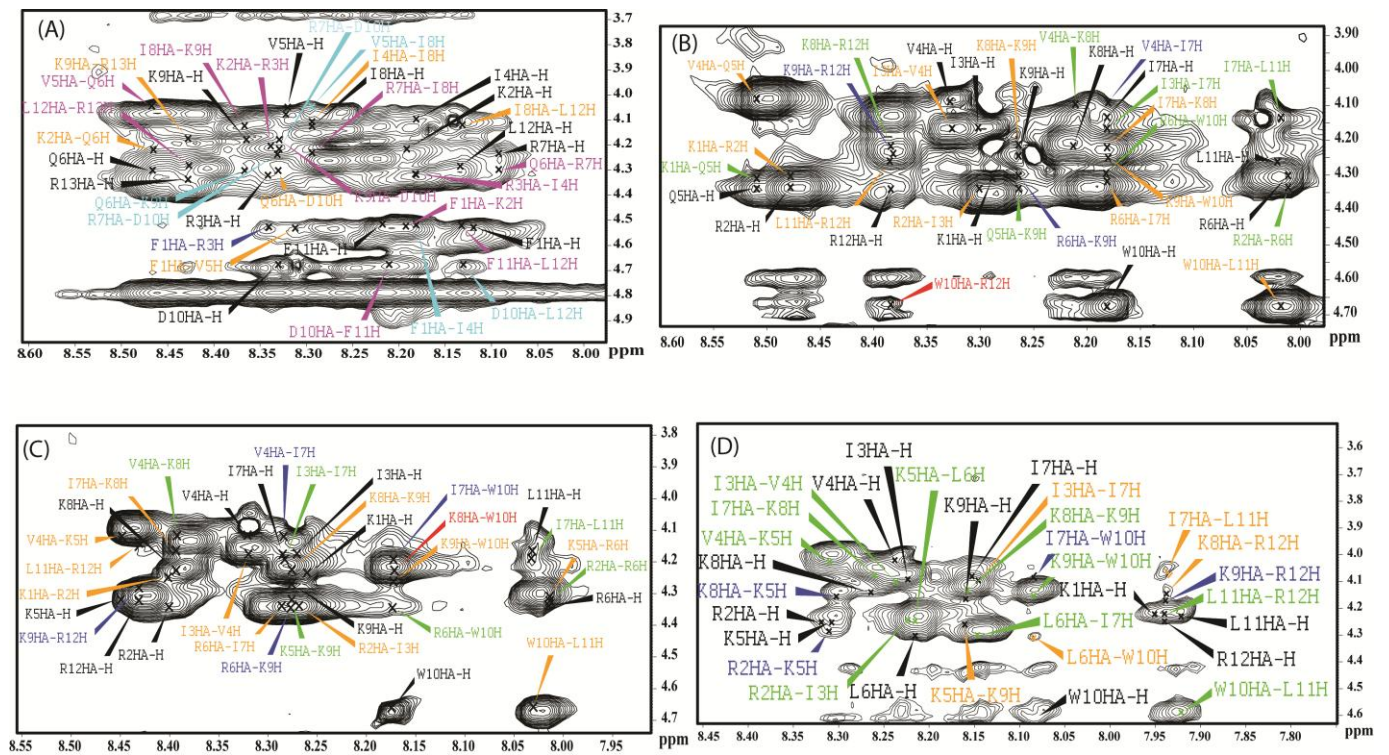


Figure S11:

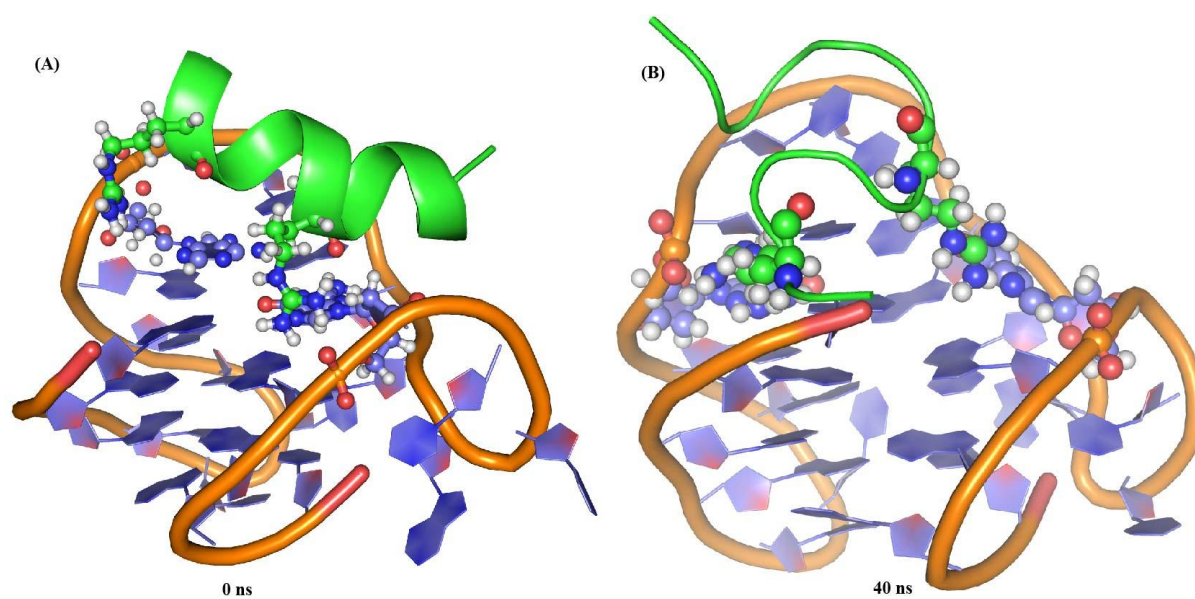


Figure S12:

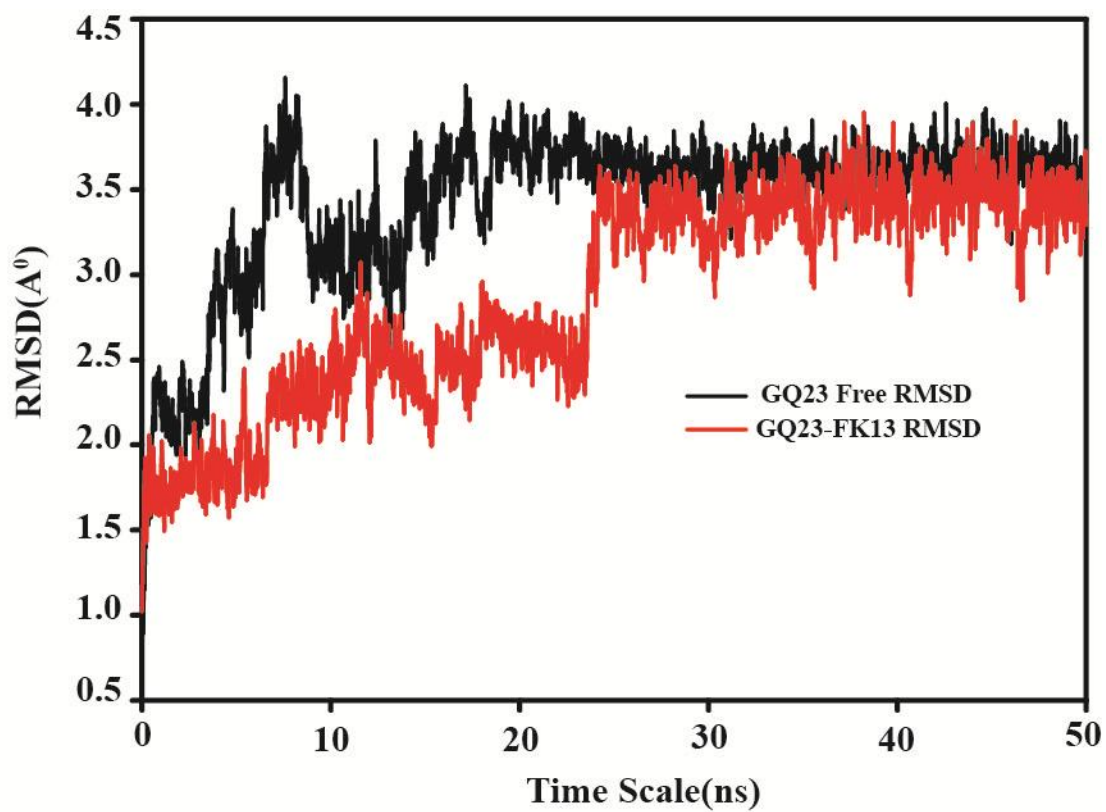


Figure S13:

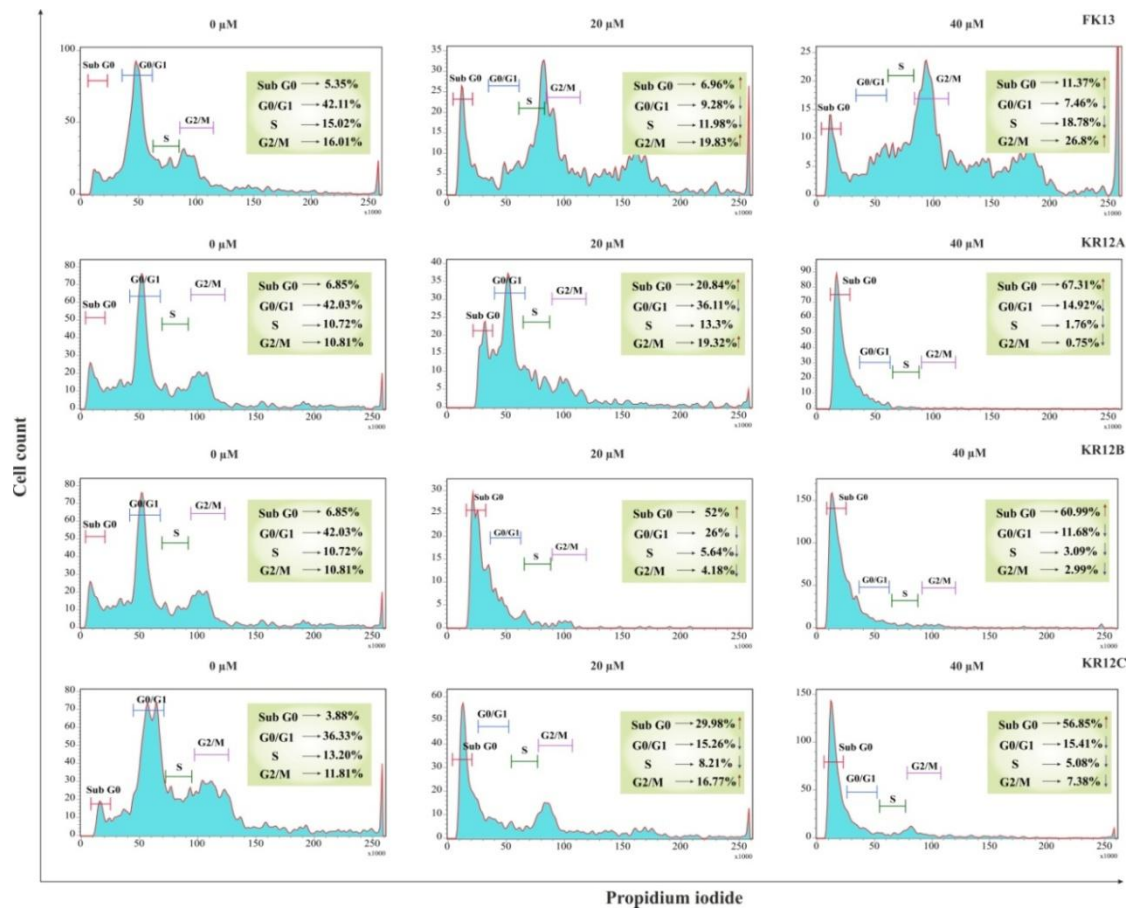


Figure S14:

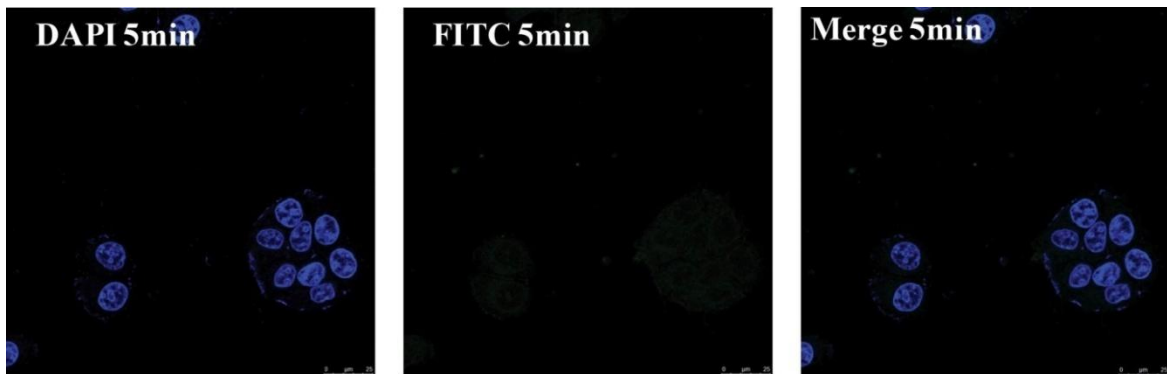


Figure S15:

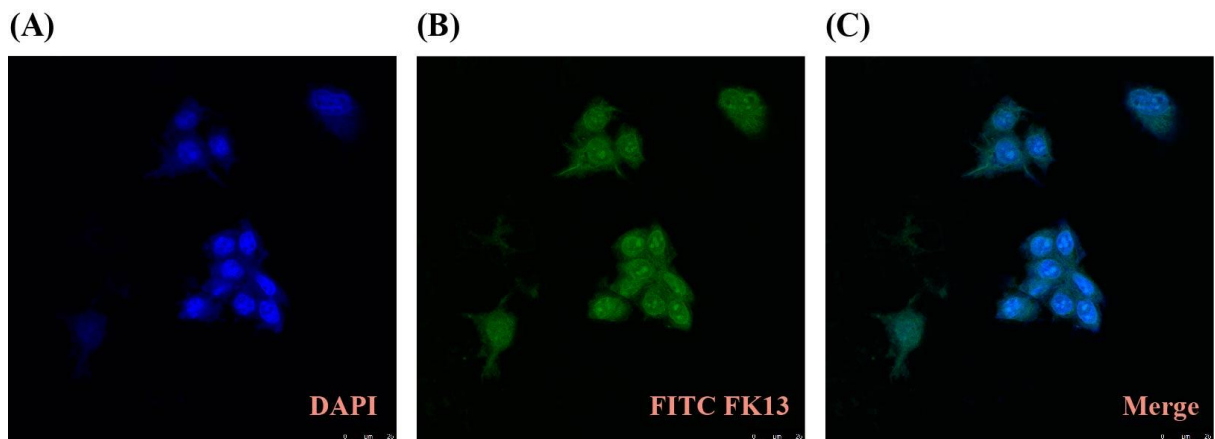


Table S1: Thermodynamic parameters obtained from ITC experiment for duplex DNA-Peptide complex.

Parameters	FK13	KR12A	KR12B	KR12C
$K_{A1}(M^{-1})$	1.2×10^4	2.1×10^4	2.2×10^4	2.3×10^4
$K_{A2}(M^{-1})$	1.6×10^4	3.4×10^3	1.7×10^3	2.6×10^4
$K_{A3}(M^{-1})$	1.1×10^4	2.9×10^4	5×10^3	2.5×10^4

Table S2: Percentage of cell viability of MCF7 cells treated with the peptides after 24 hours of incubation.

Concentration	FK13	KR12A	KR12B	KR12C
Control	100±2	100±2	100±4	100±3
20 µM	85±3	90±3	92±3	60±5
40 µM	75±3	77±3	84±3	53±4
60 µM	70±2	72±2	64±4	46±3
80 µM	67±1	58±3	60±2	42±5

Table S3: Percentage of cell viability of NKE cells treated with the peptides after 24 hours of incubation.

Concentration	FK13	KR12A	KR12B	KR12C
Control	100±0	100±0	100±0	100±0
20 µM	92±0.06	94±2	91.1±2.2	92.7±0.03
40 µM	90.1±2.7	91.1±5.9	93.6±0.03	94.4±2.7
60 µM	89.2±6.8	89.2±2.2	78.7±2	81.0±4.8
80 µM	82.9±7.9	80.2±0.03	80.0±2.7	82.9±5.9

Table S4: A Summary of Structural information for the 10 final NMR Structures of peptides in LPS micelle.

Distance restrains	FK13	KR12A	KR12B	KR12C
Intra-residue(i-j=0)	45	38	40	40
Sequential (i-j=1)	40	35	38	36
Medium-range($2 \leq i-j \leq 4$)	14	15	16	11
Long-range($i-j \geq 5$)	0	0	0	0
Total	99	88	94	87
Angular restraints				
ϕ	12	11	11	11
ψ	12	11	11	11
Distance restraints from violations (≥ 0.3)	0	0	0	0
Deviation from mean structure(A°) Average backbone to mean structure	0.42±0.16	0.33±0.09	0.35±0.10	0.42±0.16
Average heavy atom to mean structure	1.41±0.38	1.31±0.15	1.27±0.33	1.41±0.38